SAND2019-0114R

Infrasound signatures from buried chemical explosions during the SPE Phase 1

Daniel C. Bowman, Rodney Whitaker, and Philip Blom

Abstract

Strong ground motion induces acoustic waves in the atmosphere that can be detected at great distances. These waves provide a record of acceleration at the epicenter of the subterranean event. While this information is valuable for nuclear monitoring purposes, a systematic study of the variation in acoustic parameters with explosive yield and depth has not yet been conducted. Here, we provide a survey of low frequency sound waves generated during the Source Physics Phase 1 experiment, in which six chemical explosions were detonated in granite. We found that pressure amplitudes increase with explosion size but decrease with depth as expected. Pressure amplitude variability increased with signal magnitude. Surprisingly, peak frequency appears to increase with depth. A possible directional signal was identified for one of the events as well. The results presented here may aid the nuclear monitoring community in developing means of determining event depth and yield using acoustic methods. This will complement existing algorithms based on seismic radiation.

Introduction

Forces imposed on the atmosphere can create acoustic waves that may propagate over great distances. Since attenuation varies as the square of frequency, long distance acoustic recording is typically done in the "infrasound" range (<20 Hz, below human hearing). Sensitive microbarometers can detect these signals; the resulting records contain clues about the event that created the waves as well as the properties of the intervening atmosphere.

Underground explosions can generate infrasound in several ways. Pressure waves can transmit directly across the Earth/atmosphere interface despite an impedance ratio on the order of 10^{-6}. If the ground motion is sufficiently strong, subsurface layers can be subject to tensile failure and enter ballistic free fall in a phenomenon known as "spall". When these layers come to rest, the resulting sudden deceleration may create a powerful acoustic pulse. Finally, infrasound radiated from the horizontal motion of topography has been reported for earthquakes; presumably this can occur for buried explosions as well. However, it is likely to be much smaller amplitude compared to the direct transmission and spall cases.

Because the primary infrasound generation region is located at the epicenter of the event, these low frequency pressure waves offer a remote window into strong motion directly above the blast. This motion is itself related to the size and depth of the explosion. Recognizing the nuclear monitoring potential of this phenomenon, the SPE science team deployed a network of infrasound microbarometers during the SPE Phase 1 experiment. Results from the campaign indicate that emplacement depth and explosive yield do exert an influence on the amplitude and frequency content of the resulting acoustic signal. This report discusses the signals that were

recorded and their relationship to the explosions that generated them. See Table 1 for event parameters.

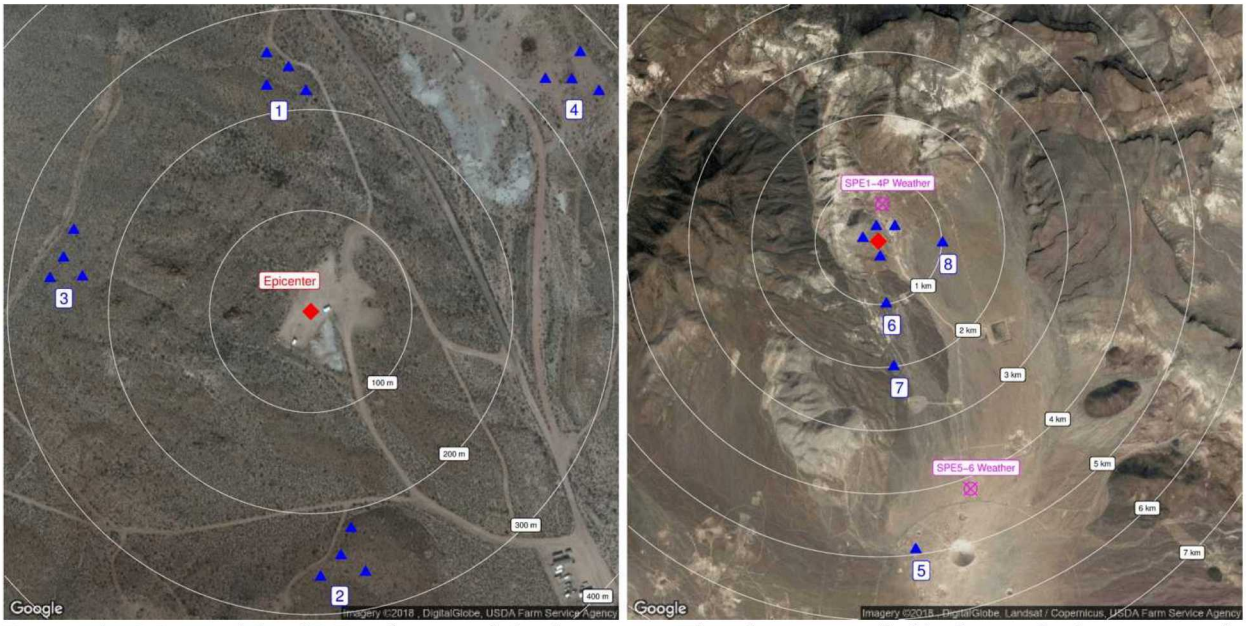

Figure 1: Maps of the SPE infrasound deployment. The close view (left) shows the locations of individual sensors for the closest four arrays. The far view shows the locations of all eight arrays.

Sensor Network

The SPE Phase 1 infrasound network consisted of arrays of Hyperion microbarometers located from 250 m to 5 km from the explosion epicenter. There was a total of 8 arrays by the end of the campaign, although not every array was active for each explosion. Four were within about 300 m, two were located at 1 km, and one was located at about 5 km from ground zero (Figure 1). The arrays consisted of four microbarometers spaced about 30 m apart. Data were recorded on a local digitizer, then telemetered offsite for archiving. Wind noise mitigation consisted of soaker hoses and shrouds. The last two experiments (SPE-5 and SPE-6) included some seismically decoupled microbarometers in the close arrays (< 300 m) to reduce the influence of sensor motion on the recorded signals.

Methods

Infrasound microbarometers are sensitive to ground motion. This is due to the instrument's sensitivity to acceleration as well as its motion through the atmospheric pressure gradient. Ground motion interference was present on all the arrays, but was a particular issue with the four closest to the epicenter since the seismic and infrasound waves arrived close together.

The ground motion signal was attenuated 2-5x when time series from each array element was aligned by maximum underpressure (the most easily identifiable part of the infrasound

signal) and then stacked. Potential acoustic arrivals from SPE-4P were identified by searching for signals that traveled at acoustic velocity, but the resulting time series still tended to be noisy.

After stacking, a 1 second window centered on maximum underpressure was extracted. A cosine (Hann) taper was applied to improve spectral resolution and to further reduce the effect of seismic noise. Amplitudes were scaled to 1 km from the epicenter by assuming that geometric attenuation was proportional to the inverse of range. Acoustic energy was calculated using specific acoustic impedance values based on temperature and pressure recorded at a weather station located inside the network. Energy was assumed to be distributed uniformly across a 1 km radius hemisphere centered on the epicenter.

Figure 2 shows waveforms from Array 3 after applying the steps outlined above. The ensemble Hilbert spectrograms were generated using the Ensemble Empirical Mode Decomposition (EEMD) method. The EEMD avoids the time/frequency resolution tradeoff of Fourier-based spectrograms. Figure 3 shows Fourier spectra of the waveforms recorded on Array 3.

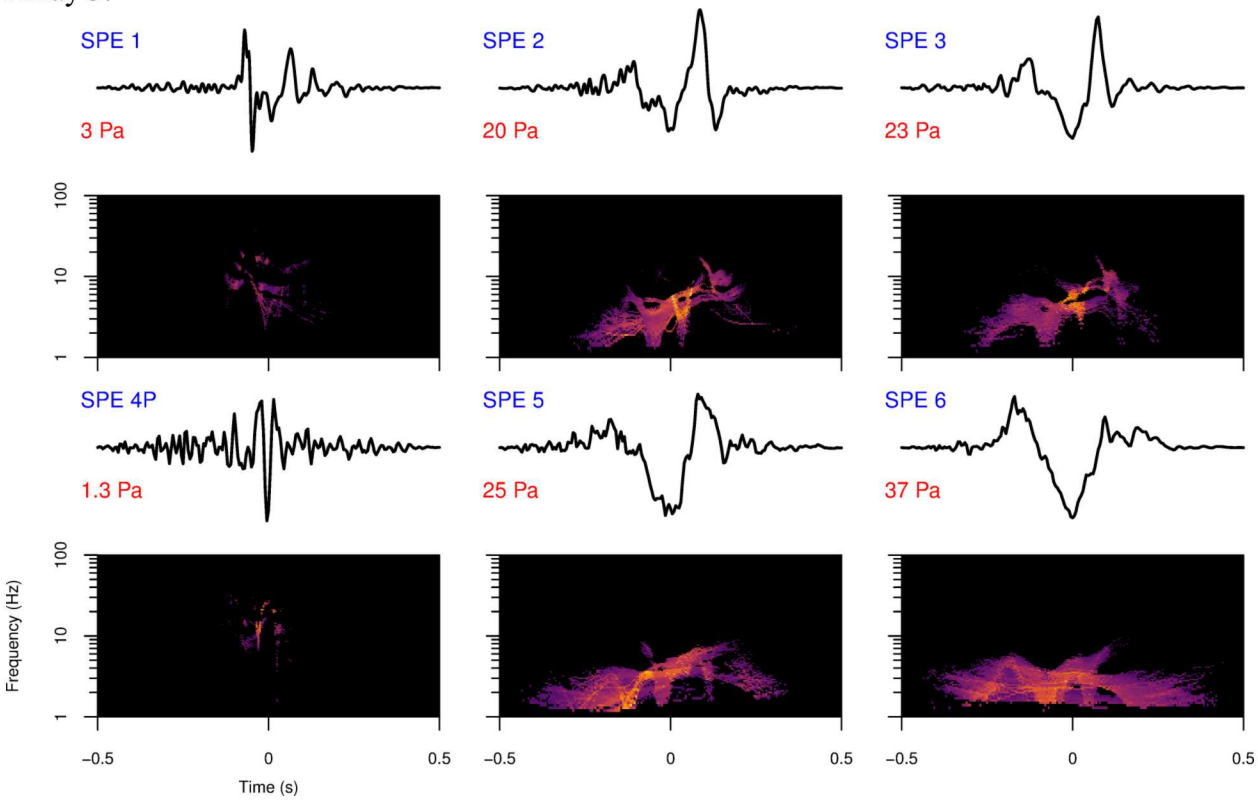

Figure 2: Waveforms and ensemble Hilbert spectrograms of infrasound recorded at Array 3. Pressure waveforms are not scaled for distance.

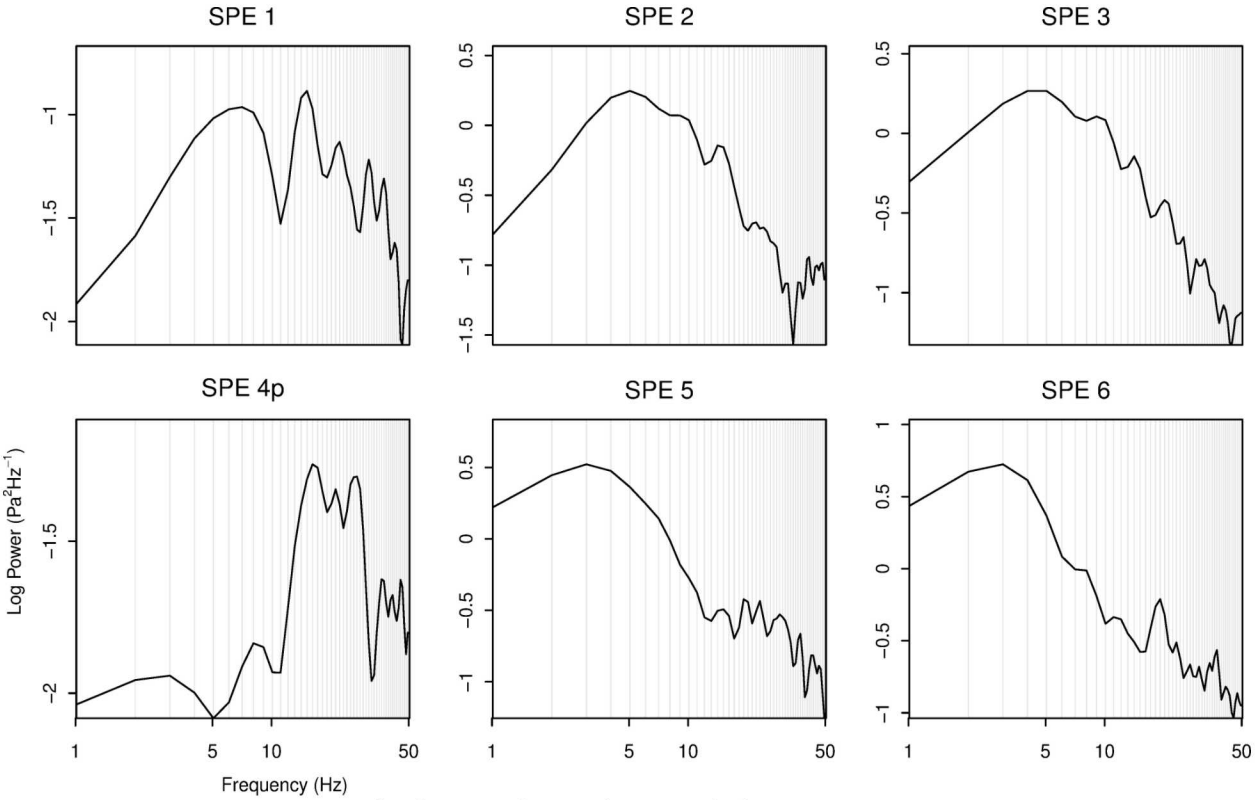

Figure 3: Fourier spectra of infrasound signals recorded at Array 3.

Results and Discussion

The SPE-1 event was small and deeply buried, resulting in a correspondingly small acoustic signal. An additional complication is that the detonating cord that initiated the blast also produced a sound wave at the ground surface. This is probably the origin of the impulsive signal seen at the beginning of the acoustic arrival in Figure 2. The amplitude of this arrival was reduced through stacking, indicating that it may have traveled at supersonic velocities (e. g. a shock wave). In any case, the reported amplitudes for this event (

While data from Arrays 1, 2, and 4 were also included in the SPE-4P analysis, it is not clear if there are any true pressure waves present. Rather, sensor motion interference dominates the pressure trace. The fact that the peak frequencies of these other arrays were in the ~30 Hz range whereas that of Array 3 was 16 Hz also argues for a fundamental difference between it and the others. The reason that only Array 3 detected a signal may be due to the highly directional nature of ground-motion induced infrasound. Sound waves will tend to have much higher amplitude directly above the epicenter than to the side if the deforming region is a significant fraction of the acoustic wavelength. Array 3 is located on a hillslope at an elevation angle of approximately 10° with respect to ground zero. It may be this was sufficient to capture a more powerful wave compared to the stations that were more coplanar with the source. At present this conclusion is speculative; it would benefit from a focused study that also examined the other 5 events for similar directivity effects.

SPE-5 had the largest explosive yield, but it was also the second deepest shot. SPE-6 had approximately half the yield of SPE-5, but was also at about half the depth. The average

amplitude and frequency content of the two events were approximately equal, although the waveforms are not as similar as those between SPE-2 and SPE-3 (Figure 2).

Basic physical reasoning suggests that radiated acoustic energy should depend on both the size and depth of the buried explosion. The scaled depth of burial (SDOB), defined as depth divided by explosive yield to the 1/3 power, is commonly used to compare buried explosions. However, even this parameter cannot be extended to all situations: a small charge buried at a shallow depth may have the same SDOB as a large charge buried deeper, but the characteristics of the resulting acoustic wave will be different. Extending relationships between SDOB and observed signal characteristics for the SPE explosions to other depth/yield combinations is risky. The effect of varying substrates (e. g. hard rock vs. alluvium) is not well understood either. However, detonating two charges in the same location (SPE-2 and SPE-3) seems to result in very similar waveforms, indicating that near-source damage effects have little influence on the acoustic signal.

Table 1) are probably biased high. This arrival probably contributed to a prominent spectral peak above 10 Hz (Figure 3), which is not included in

While data from Arrays 1, 2, and 4 were also included in the SPE-4P analysis, it is not clear if there are any true pressure waves present. Rather, sensor motion interference dominates the pressure trace. The fact that the peak frequencies of these other arrays were in the ~30 Hz range whereas that of Array 3 was 16 Hz also argues for a fundamental difference between it and the others. The reason that only Array 3 detected a signal may be due to the highly directional nature of ground-motion induced infrasound. Sound waves will tend to have much higher amplitude directly above the epicenter than to the side if the deforming region is a significant fraction of the acoustic wavelength. Array 3 is located on a hillslope at an elevation angle of approximately 10° with respect to ground zero. It may be this was sufficient to capture a more powerful wave compared to the stations that were more coplanar with the source. At present this conclusion is speculative; it would benefit from a focused study that also examined the other 5 events for similar directivity effects.

SPE-5 had the largest explosive yield, but it was also the second deepest shot. SPE-6 had approximately half the yield of SPE-5, but was also at about half the depth. The average amplitude and frequency content of the two events were approximately equal, although the waveforms are not as similar as those between SPE-2 and SPE-3 (Figure 2).

Basic physical reasoning suggests that radiated acoustic energy should depend on both the size and depth of the buried explosion. The scaled depth of burial (SDOB), defined as depth divided by explosive yield to the 1/3 power, is commonly used to compare buried explosions. However, even this parameter cannot be extended to all situations: a small charge buried at a shallow depth may have the same SDOB as a large charge buried deeper, but the characteristics of the resulting acoustic wave will be different. Extending relationships between SDOB and observed signal characteristics for the SPE explosions to other depth/yield combinations is risky. The effect of varying substrates (e. g. hard rock vs. alluvium) is not well understood either. However, detonating two charges in the same location (SPE-2 and SPE-3) seems to result in very

similar waveforms, indicating that near-source damage effects have little influence on the acoustic signal.

Table 1 for that reason. SPE-2 and SPE-3 were similar in size and emplacement depth. As a result, their waveforms and frequency content are quite similar. SPE-4P was the smallest and deepest explosion in the series. The existence of a detectable acoustic pulse from this event is difficult to verify due to interference from seismic noise. Wavelets traveling at acoustic speeds were recorded on Array 3; the resulting combined signal exhibits a single arrival. The wavelet's underpressure has a greater magnitude than its overpressure, similar to those recorded on SPE-5 and SPE-6.

While data from Arrays 1, 2, and 4 were also included in the SPE-4P analysis, it is not clear if there are any true pressure waves present. Rather, sensor motion interference dominates the pressure trace. The fact that the peak frequencies of these other arrays were in the ~30 Hz range whereas that of Array 3 was 16 Hz also argues for a fundamental difference between it and the others. The reason that only Array 3 detected a signal may be due to the highly directional nature of ground-motion induced infrasound. Sound waves will tend to have much higher amplitude directly above the epicenter than to the side if the deforming region is a significant fraction of the acoustic wavelength. Array 3 is located on a hillslope at an elevation angle of approximately 10° with respect to ground zero. It may be this was sufficient to capture a more powerful wave compared to the stations that were more coplanar with the source. At present this conclusion is speculative; it would benefit from a focused study that also examined the other 5 events for similar directivity effects.

SPE-5 had the largest explosive yield, but it was also the second deepest shot. SPE-6 had approximately half the yield of SPE-5, but was also at about half the depth. The average amplitude and frequency content of the two events were approximately equal, although the waveforms are not as similar as those between SPE-2 and SPE-3 (Figure 2).

Basic physical reasoning suggests that radiated acoustic energy should depend on both the size and depth of the buried explosion. The scaled depth of burial (SDOB), defined as depth divided by explosive yield to the 1/3 power, is commonly used to compare buried explosions. However, even this parameter cannot be extended to all situations: a small charge buried at a shallow depth may have the same SDOB as a large charge buried deeper, but the characteristics of the resulting acoustic wave will be different. Extending relationships between SDOB and observed signal characteristics for the SPE explosions to other depth/yield combinations is risky. The effect of varying substrates (e. g. hard rock vs. alluvium) is not well understood either. However, detonating two charges in the same location (SPE-2 and SPE-3) seems to result in very

similar waveforms, indicating that near-source damage effects have little influence on the acoustic signal.

Table 1: Acoustic properties of the SPE events.

Event	Date	Depth	Yield	SDOB	Amplitude	Amplitude	Frequency	Energy
	UTC	m	kg TNT eq.	m * $kt^{-1/3}$	Pa P2P	Pa RMS	Hz	Log_{10} J
SPE-1	5/3/2011 22:00:00	55.1	90	980	1.1 ± 0.60	0.078 ± 0.027	7.5 ± 0.58	4.7 ± 0.13
SPE-2	10/25/2011 19:00:00	45.7	1000	360	3.6 ± 0.97	0.54 ± 0.13	4.9 ± 0.41	6.7 ± 0.27
SPE-3	7/24/2012 18:00:00	47.2	910	390	3.2 ± 1.4	0.49 ± 0.16	4.3 ± 0.90	6.6 ± 0.38
SPE-4P	5/21/2015 18:36:00	87.2	89	1600	0.23 ± 0.059	0.028 ± 0.0044	27 ± 6.9	2.9 ± 0.2
SPE-5	4/26/2016 20:49:00	76.5	5000	350	7.1 ± 2.7	1.2 ± 0.45	2.9 ± 0.36	7.2 ± 0.29
SPE-6	10/12/2016 18:36:00	31.4	2200	190	7 ± 1.6	1.3 ± 0.19	2.5 ± 0.54	7 ± 0.2

Peak to peak (P2P) amplitude is defined here as the range between the maximum overpressure and maximum rarefaction, often within one cycle. It is clearly sensitive to both explosion size and depth. The SPE-2 shot was 10x larger than SPE-1 and at a slightly shallower depth. As a result, the P2P amplitude is over three times as large. The P2P amplitude for SPE-1 is nearly five times that of SPE-4P despite both having nearly the same explosive charge. SPE-4P was buried 1.6 times as deep as SPE-1, resulting in less energy crossing the Earth/atmosphere barrier. However, it is important to recall that the amplitude of SPE-1 may have been augmented from the detonation cord exploding at the surface. The true amplitude ratio may be lower.

P2P amplitude is a variable metric because it is measured across two precise points in the time series (the maximum and minimum). Background noise fluctuations can have a large impact on these points, especially when the signal to noise ratio is poor. Root mean square (RMS) amplitude encodes both amplitude and frequency, and also reduces the impact of spurious signal fluctuations. The RMS amplitude ratio between SPE-2 and SPE-1 is now a factor of 7; perhaps a more realistic measure since the initial acoustic pulse from the detonation cord has been deemphasized. In contrast, the ratio between SPE-1 and SPE-4P is now less. Despite these differences, RMS amplitude follows a similar trend of increasing with explosion size and decreasing with depth.

The frequency content of infrasound signals is a useful metric because it is less sensitive to atmospheric variations that can result in large amplitude discrepancies at ranges of only a few kilometers. Peak frequency scales inversely with explosion size for aerial blasts. The same appears approximately true for the SPE series as well. The smallest shots (SPE-1 and SPE-4P) had the highest frequencies, and the largest shots (SPE-5 and SPE-6) had the lowest. However, SPE-6 had the lowest frequency despite being less than half the size of SPE-5. SPE-1 had a peak frequency of 7.5 Hz and SPE-4P had a peak frequency of 16 Hz on Array 3, despite the two

shots being approximately equal in size. This suggests that deeper explosions tend to produce higher frequency infrasound, all other things being equal.

This seemingly counterintuitive result may be a consequence of the infrasound directivity problem described earlier. A deeper explosion creates a correspondingly smaller region of ground motion with sufficient amplitude to produce a far field acoustic signal. In turn, this allows shorter wavelength (and hence higher frequency) signals to escape in the horizontal direction. If this is true, a sensor placed directly above the epicenter would see essentially no difference in spectral shape for two explosions of equivalent size buried at different depths.

Acoustic energy scales quadratically with pressure amplitude and frequency. In Table 1, the quantity reported (last column) is not the true energy release, since that can only be quantified using sensors at multiple elevation angles distributed around the epicenter. Rather, it is a measure of the energy generated by an "acoustically compact" (isotropically radiating) equivalent source. Also, the significant topography around the epicenter may affect the recorded energy values. This is not a concern for inter-SPE comparisons since the position of the detectors and the source remained static relative to the topography. Finally, energy is only reported in the 1-10 Hz band in Table 1 and Figure 1 to avoid contamination from seismic noise.

Despite these caveats, some general patterns can be discerned. Depth exerts a strong control on energy release; SPE-5 and SPE-6 have nearly identical values despite the former being twice the size of the latter. However, SPE-2 is an order of magnitude larger than SPE-1 and only 10 meters shallower, yet releases two orders of magnitude more energy.

Signal parameter distributions also reveal details about the acoustic phenomenology across the SPE series (Figure 4). The variance of the amplitude-based metrics (P2P amplitude, RMS amplitude, and energy) became greater with increasing values. This is consistent with possible signal directivity due to source effects (uneven acoustic radiation near the epicenter), reflections from topography, and atmospheric variations. All of these should produce an approximately linear scaling with amplitude. On the other hand, peak frequency values tended to vary relatively little between arrays, underscoring the relative insensitivity of the signal's spectral content to the perturbing factors mentioned above. The one major exception is SPE-4P; this may be due to directivity and seismic noise contamination as was discussed earlier.

The depth and explosive yield effects on amplitude-based metrics is clear in Figure 4 as well. Each successive SPE explosion has a decreasing SDOB, with the exception of SPE-4P; P2P and RMS amplitude increase in concert with this. The peak frequency plot shows the reverse: the smallest and deepest explosion has the highest frequency, whereas the explosions with the smallest SDOB have the lowest frequency.

Conclusions

The SPE Phase 1 represented a unique opportunity to investigate acoustic signals generated by buried explosions in hard rock. All of the six shots generated infrasound signals that were recovered on at least one of eight arrays deployed near the epicenter. Infrasound waveforms varied considerably across the series, but the two explosions with nearly identical yields and emplacement depths created correspondingly similar signals. Amplitude-based metrics decreased with increasing depth but grew stronger for larger explosions as expected. Peak frequencies decreased with explosion size, but also appeared to increase for deeper explosions. Evidence for possible signal directivity was found for the SPE-4P event. Signal

amplitude variation increased with increasing magnitude, but the spread in peak frequency values appeared relatively constant across all six shots.

Acknowledgments

The Source Physics Experiments (SPE) would not have been possible without the support of many people from several organizations. The authors wish to express their gratitude to the National Nuclear Security Administration, Defense Nuclear Nonproliferation Research and Development (DNN R\&D), and the SPE working group, a multi-institutional and interdisciplinary group of scientists and engineers.

Sandia National Laboratories is a multi-mission laboratory managed and operated by National Technology and Engineering Solutions of Sandia, LLC., a wholly owned subsidiary of Honeywell International, Inc., for the U.S. Department of Energy's National Nuclear Security Administration under contract DE-NA0003525. The views expressed here do not necessarily

reflect the views of the United States Government, the United States Department of Energy, or Sandia National Laboratories.

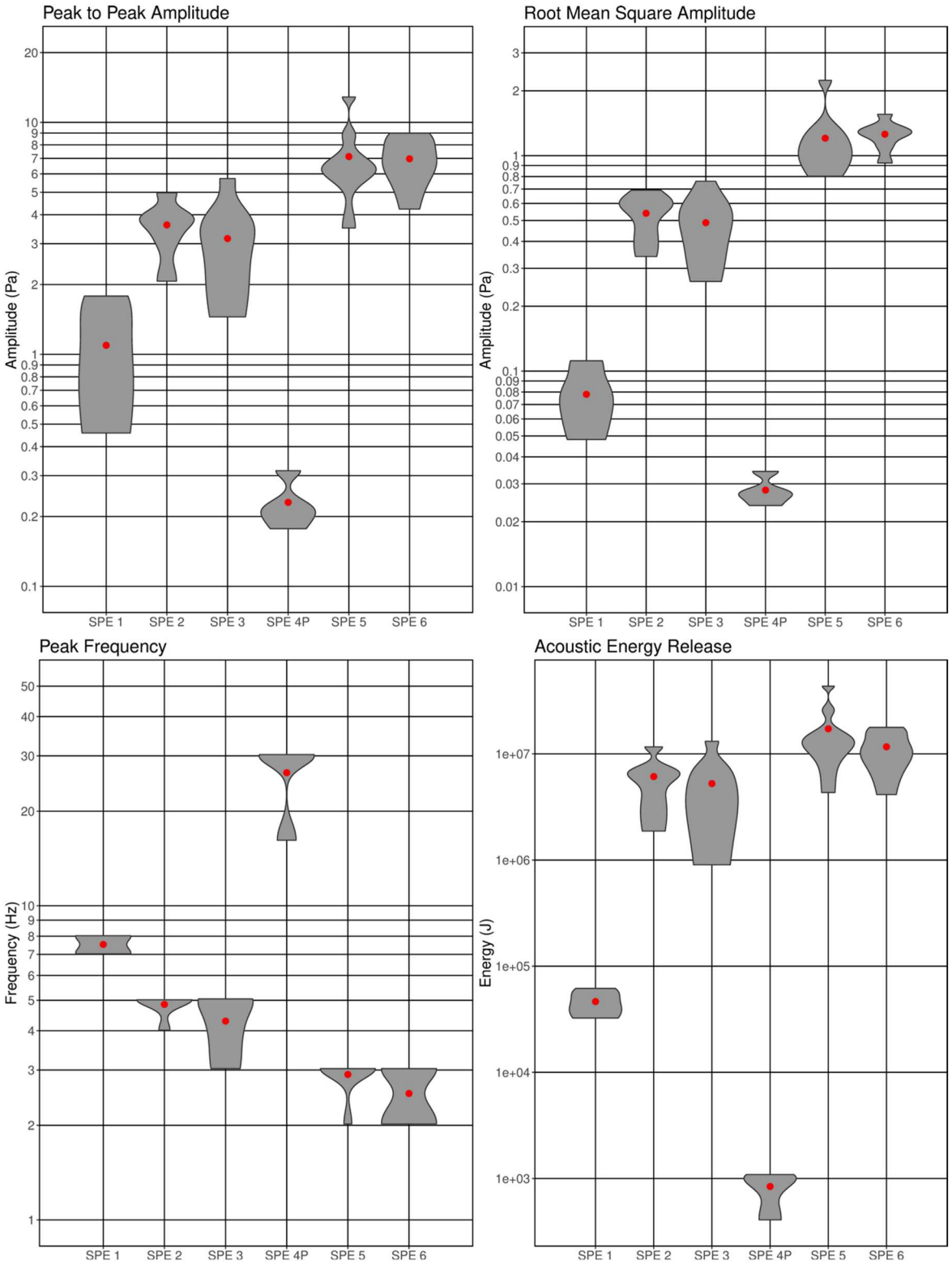

Figure 4: Violin plots of signal characteristics recorded across the infrasound network for each shot. Amplitudes have been scaled to 1 km from the source. Red dots denote the mean of each data set. Plots are truncated beyond the range of the most extreme data points.